

## SYNTHESIS OF SMALL CRYSTALS ZEOLITE NaX BY A ULTRASONIC AGING METHOD

X. ZHANG\*, S. LI, G. ZHANG

*College of Chemistry and Chemical Engineering, Xuchang University, Xuchang, 461000, China*

Small crystals zeolite NaX were synthesized by applying a ultrasonic aging method, where the hydrogel was aged with ultrasound for various times, followed hydrothermally treated at 353 K for 12 hours. The products were characterized by XRD, FTIR, SEM, particle size analysis and N<sub>2</sub> adsorption-desorption technique. The results showed that ultrasonic-assited aging resulted in the samples synthesized with smaller particle sizes and narrower particle size distributions as compared with that of samples obtained with static aging. The longer the ultrasonic aging time, the smaller the particle sizes and the narrower particle size distributions will be. Moreover, ultrasonic aging time was very sensitive for zeolite composition, the Si/Al molar ratios of zeolites NaX were tested to be 1.24, 1.29, 1.35, 1.42 and 1.48 for the ultrasonic aging time of 10, 20, 30, 40 and 60 min, respectively.

(Received January 29, 2019; Accepted August 21, 2019)

*Keywords:* Zeolite NaX, Aging, Ultrasound Crystal size

### 1. Introduction

Zeolites are porous crystalline aluminosilicates of SiO<sub>4</sub><sup>4-</sup> and AlO<sub>4</sub><sup>5-</sup> tetrahedra connected by oxygen bridges [1,2]. The existence of uniformly distributed channels and cavities in molecular dimensions, typically in the size range of 0.3–1 nm approximately, endows zeolites with unique molecular discrimination, organization and recognition properties [3]. Zeolites have been widely used as ion-exchangers, adsorbents and catalysts, because of their high ion exchange capacity, superior thermal/hydrothermal stability and good shape-selectivity [4-6].

Most of applications of zeolites are closely related to their framework. However, shape and particulate properties of zeolite crystals also play a significant role in the mode and efficiency of their application [7,8]. More recently, many attempts are focused on the studies of various factors which control the particulate properties and crystallization pathway of the final products. The results show that aging process of the reaction mixture is one of the most important factors for controlling the zeolite particulate properties [9,10]. Alfaro et al. [11] have reported the synthesis of LTA zeolite in the absence of organic template. They revealed that aging had an important effect on gel chemistry, which affected nucleation, and crystal growth kinetics of zeolites. The samples synthesized with short aging time was amorphous material, while the samples obtained with aging time of 72 and 144 h were well-crystallized LTA zeolite crystals. Similar effect was observed by Kovo and Holmes [12]. In a more detail study, they revealed that aging led to an increase in the dissolution of the silicate anion during the reaction with alkali presented in the reaction mixture, thus increasing the crystallinity of zeolite. Also, Rigo et al. [13] have reported that aging influenced the crystal growth process, the ZK4 zeolite synthesized with 24 h aging at room temperature exhibited an edge size of approximately 5 μm, whereas the sample synthesized without the aging step showed an edge size of approximately 1 μm. In addition, Samadi-Maybodi et al. [14] reported the synthesis of zeolite-P via microwave assisted aging method, the results showed that aging treatment promoted the nucleation greatly, the microwave-assisted aging reduced reaction time by at least 83% compared with the conventional hydrothermal synthesis.

---

\*Corresponding author: zxxz5973428@163.com

Herein, we reported on the synthesis of crystals zeolite NaX by applying an ultrasonic aging method, where the hydrogel was aged in an ultrasonic water bath for various times, followed by hydrothermal treatment at 353 K for 12 hours. The shapes and sizes of samples synthesized via ultrasonic-assisted aging were compared to those of samples synthesized under conventional hydrothermal methods. Moreover, the ultrasound-assisted aging mechanism was also proposed.

## 2. Methods

### 2.1. Zeolite synthesis

In a typical synthesis, 24.8 g of sodium hydroxide (99%, Merck) was dissolved in 103.7 ml of deionized water, followed by addition of 10.2 g of sodium aluminate (anhydrous, Sigma-Aldrich) to get a clear solution. 35.0 g of 30 wt.% aqueous colloidal silica (Ludox HS-30, Sigma-Aldrich) was weighed and slowly poured into the above solution under vigorous stirring (800 rpm), the molar composition of the resultant mixture was 6.0 Na<sub>2</sub>O:1.0 Al<sub>2</sub>O<sub>3</sub>:2.8 SiO<sub>2</sub>:114 H<sub>2</sub>O. Two different sets of synthesis experiments were performed through (i) a conventional hydrothermal process; the mixture was transferred to a water bath (313 K) and aged for 60 min under static conditions, then hydrothermally treated at 353 K for 12 hours, the synthesized sample was denoted A-60. (ii) a hydrothermal process preceded by ultrasonication; the mixture was aged in an ultrasonic water bath (313 K, 35 kHz), the temperature of the ultrasonic water bath was controlled by using a heater and a temperature controller. 20 ml of the resultant creamy hydrogel was taken with different aging times, i.e., 10, 20, 30, 40, and 60 min, then transferred to polypropylene bottles, sealed and placed in a convection oven, hydrothermally treated at 353 K for 12 hours. The synthesized samples were then denoted U-10, U-20, U-30, U-40 and U-60. For comparison, the experiment was performed in which sample was synthesized after 60 min ultrasonic aging, without further hydrothermal treatment, the sample obtained was denoted H-0.

After synthesis, all the solid samples were filtered off, thoroughly washed with deionized water and dried at 373 K overnight.

### 2.2. Characterization and Analyses

XRD patterns were obtained on a Philips APD-3720 diffractometer with Cu K $\alpha$  radiation, operated at 20 mA and 40 kV. The diffraction patterns were collected in the 2 $\theta$  range of 5–40° at a scan speed of 0.05° 2 $\theta$ /min. Transmission IR spectra were recorded by a JASCO Fourier transform infrared spectrometer with a resolution of 4 cm<sup>-1</sup> using a KBr method. SEM images were obtained on a JEOL JSM-6700F microscope equipped with a cold-field emission gun, operating at 2 kV and 10  $\mu$ A. Particle size distribution curves of samples were measured with a Malvern Mastersizer 2000 laser light-scattering particle size analyzer, the solution was ultrasonicated for 40 min before the measurement. Elemental Si/Al ratio of sample was determined by atomic absorption spectroscopy analysis on a WFX-1C spectrometer. Nitrogen adsorption-desorption experiments were carried out at 77 K on a Micrometrics ASAP 2020 sorption analyzer, all samples were degassed prior to each measurement.

## 3. Results and discussion

The XRD patterns of samples obtained from different synthesis processes are shown in Fig. 1. As shown in Fig. 1a–f, the synthesized products match the characteristic peaks of FAU zeolite-type structure at 2 $\theta$  values of 6.2°, 10.1°, 11.9°, 15.5°, 18.6°, 20.2°, 23.6°, 26.7°, 29.5°, 31.0°, 33.9° and 37.7° that were reported by Nibou and Amokrane [15], suggesting successful synthesis of FAU zeolite with good crystallinity. However, it is also noted that the XRD diffraction peaks of samples obtained with longer aging time in the presence of ultrasound (40 and 60 min) are relatively broad, indicating that the products consist of small crystals. In contrast, the peaks of samples with 10, 20 and 30 min ultrasonic aging and 60 min static aging do not suggest small particle sizes. Fig. 1g displays that the sample obtained without hydrothermal treatment after 60 min ultrasonic aging is totally amorphous. These important observations confirm that hydrothermal treatment process is necessary to synthesize FAU zeolite, the application of ultrasound at the aging stage decreases the crystal size of the synthesized samples.

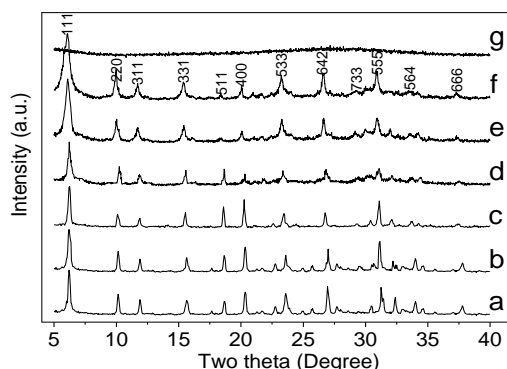


Fig. 1. XRD patterns of samples obtained from different synthesis processes. Sample A-60 (a), U-10 (b), U-20 (c), U-30 (d), U-40 (e), U-60 (f) and H-0 (g).

The spectra of samples H-0, U-10, U-20 and U-60 are shown in Fig. 2. As a result, sample H-0 does not show characteristic FAU adsorption bands, indicating it is still amorphous sodium aluminosilicate (Fig. 2a). IR spectra of the samples obtained with hydrothermally treated after 10, 20 and 60 min ultrasonic aging clearly show three FAU characteristic bands, which are double-ring vibration at  $562\text{ cm}^{-1}$  and symmetric stretching bands at  $684\text{ cm}^{-1}$  and  $760\text{ cm}^{-1}$  (Fig. 2b-d), confirming the samples are highly crystalline FAU zeolite [16,17]. Moreover, it can be seen that the absorption bands at around  $1442\text{ cm}^{-1}$  and  $1356\text{ cm}^{-1}$  are disappeared for samples U-10, U-20 and U-60, this can be explained that the progressive phase transformation of amorphous phase into crystalline FAU phase [18,19]. These results are in good agreement with the XRD results.

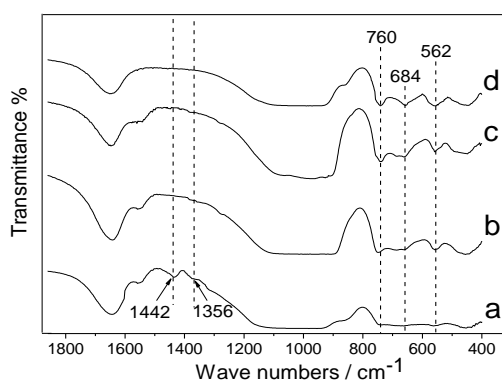


Fig. 2. FT-IR spectra of samples H-0 (a), U-10 (b), U-20 (c) and U-60 (d).

The SEM micrographs and corresponding particle size distributions of samples A-60, U-10, U-20, U-30, U-40 and U-60 are shown in Fig. 3 and Fig. 4, respectively. From Fig. 3, isolated particles with a round shape samples could be obtained after hydrothermally treated, and the samples obtained with long ultrasonic aging time show smaller particle sizes, as expected. For sample U-40 and U-60, SEM micrographs exhibit that the samples are composed of a large number of relatively uniform spherical particles with an average size of 100 nm approximately. This observation agrees well with the XRD results, in which relatively broad characteristic FAU diffraction patterns are observed [20]. As shown in Fig. 4, the samples A-60, U-10, U-20, U-30, U-40 and U-60 show the average particle sizes of 878, 946, 312, 202, 102 and 100 nm, and the particle size distribution ranges of 750–1028, 802–1136, 198–412, 104–308, 95–120 and 96–112 nm, respectively.

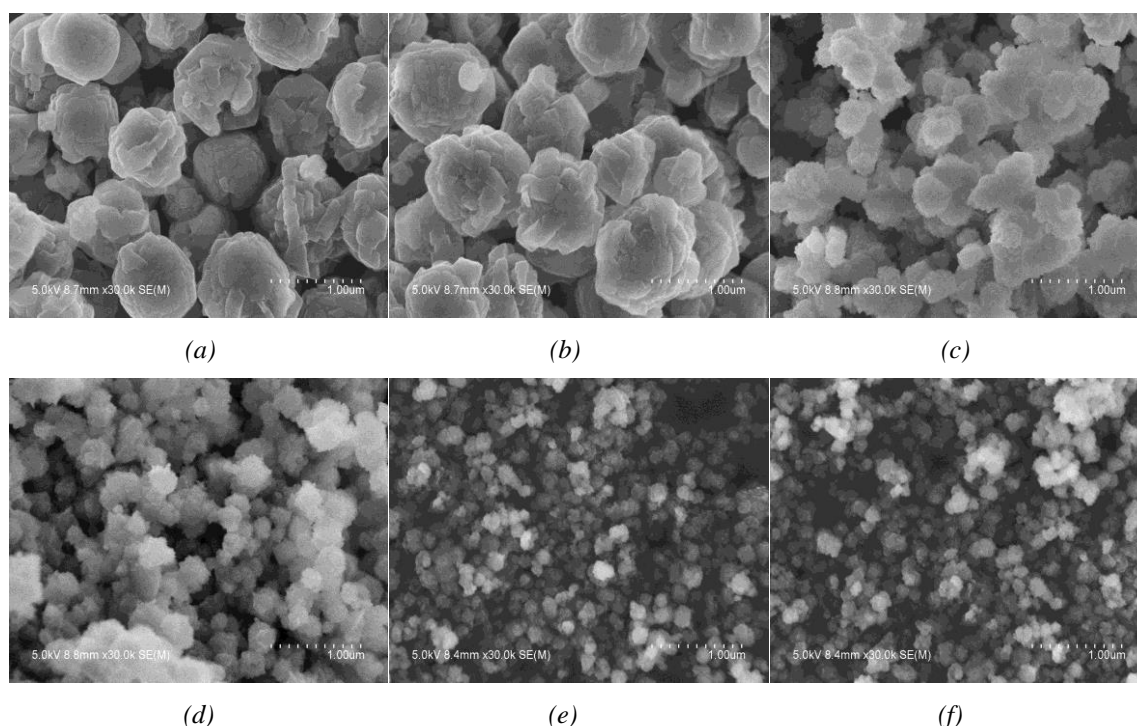


Fig. 3. SEM pictures of samples A-60 (a), U-10 (b), U-20 (c), U-30 (d), U-40 (e) and U-60 (f).

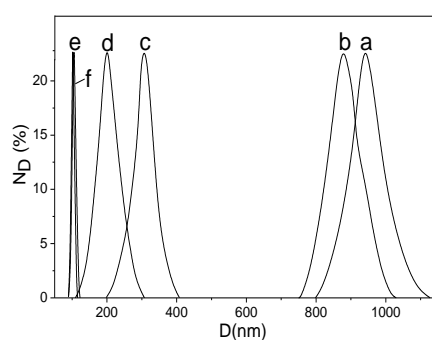


Fig. 4. Particle size distribution curves of samples A-60 (a), U-10 (b), U-20 (c), U-30 (d), U-40 (e) and U-60 (f).

The  $N_2$  adsorption-desorption results and Si/Al molar ratios of as-synthesized FAU zeolite particles are listed in Table 1. Clearly, for a similar gel composition, the sample synthesized using an aging pretreatment with ultrasound (U-60) are shown to exhibit larger BET and external surface area than sample obtained employing static aging (A-60) with the same aging time. Moreover, the longer the ultrasonic aging time, the larger BET and external surface area will be. The BET surface areas of FAU zeolite samples increase from 440 to 664  $m^2/g$  while the ultrasonic aging time increase from 10 to 60 min. The corresponding external surface area shows a similar trend, i.e., it increases from 121  $m^2/g$  for sample U10 to 132  $m^2/g$  for sample U60. These results are in correspondence with smaller particle size and narrower particle size distributions. In our study, with the increase of ultrasonic aging time from 10 to 60 min, the Si/Al molar ratios of samples obtained are tested to be 1.24, 1.29, 1.35, 1.42 and 1.48 for U-10, U-20, U-30, U-40 and U-60, respectively. The Si/Al molar ratios of samples obtained are 1.24–1.48, which are in the range of zeolite NaX.

Table 1.  $N_2$  adsorption-desorption results and Si/Al molar ratios of as-synthesized FAU zeolite particles.

Samples	$S_{\text{BET}}$ ( $\text{m}^2/\text{g}$ )	$S_{\text{external}}$ ( $\text{m}^2/\text{g}$ )	$V_{\text{micropore}}$ ( $\text{cm}^3/\text{g}$ )	$V_{\text{total}}$ ( $\text{cm}^3/\text{g}$ )	Si/Al molar ratio of sample
A-60	450	121	0.27	0.35	1.22
U-10	440	121	0.27	0.36	1.24
U-20	602	125	0.28	0.38	1.29
U-30	616	129	0.30	0.39	1.35
U-40	660	132	0.32	0.41	1.42
U-60	664	132	0.32	0.42	1.48

From the above results, the present study clearly reveals that ultrasonic-assisted aging results in the samples synthesized with smaller particle sizes and narrower particle size distributions as compared with that of samples obtained with static aging. Also, the longer the ultrasonic aging time, the smaller the particle size and the narrower particle size distributions will be. For the ultrasonic-assisted aging, we assume that the sonication is acoustic cavitation that generates high energy shock waves, thus increases the nucleation rates, and the subsequent high temperature is favorable for the crystal growth [21]. Therefore, the fast nucleation at the aging stage in the presence of ultrasound allows the formation of a large quantity of crystal nuclei, the prolongation of ultrasonic aging time strongly promotes nucleation process and increases the number of nuclei in the gel matrix, which provides a favorable option for the following crystallization stage. Also, Yousefi et al. [22] have pointed that the aging step prior to crystallization substantially affected the crystal size by the increase in the number nuclei. On the other hand, Caballero et al. [23] reported that the aging time was inversely proportional to the nucleation time, too short aging time led to the occurrence of undesired nucleation of the competing phase, which hampered the crystallization of zeolite samples. While in this study, no peak of other phase or amorphous material is detected in the end products. In addition, the ultrasonic aging time is very sensitive for zeolite composition. The Si/Al molar ratio in framework is gradually increased with increasing sonication aging time. This could be attributed to the fact that sonication energy increases the concentration of soluble silicate species, thus enabling their incorporation into tetrahedrally coordinated framework [24].

#### 4. Conclusions

In summary, the ultrasonic-assisted aging results in the samples synthesized with smaller particle sizes and narrower particle size distributions. The longer the ultrasonic aging time, the smaller the particle size and the narrower particle size distributions will be. The reasons may be due to that sonication is acoustic cavitation that generates high energy shock waves, thus increases the nucleation rates. The increase of ultrasonic aging time allow more uniform nucleation to occur through the gel matrix, which assist the formation of zeolite crystals with small sizes and narrow size distributions. In addition, ultrasonic aging time is very sensitive for zeolite composition, the Si/Al molar ratio of zeolite NaX synthesized is gradually increased with increasing sonication aging time.

#### Acknowledgments

This work was supported by the College Natural Science Foundation of Henan Province (17B530004).

## References

- [1] A. Dyer, *An Introduction to Zeolite Molecular Sieve*, John Wiley, London, 1988.
- [2] R. M. Barrer, *Zeolites and Clay Minerals as Sorbents and Molecular Sieves*, Academic Press, London, 1978.
- [3] V. P. Valtchev, K. N. Bozhilov, *J. Phys. Chem. B* **108**, 15587 (2004).
- [4] A. M. Cardoso, A. Paprocki, L. S. Ferret, C. M. N. Azevedo, M. Pires, *Fuel* **139**, 59 (2015).
- [5] D. Matei, B. Doicin, D.L. Cursaru, *Dig. J. Nanomater. Bios.* **11**, 443 (2016).
- [6] D. L. Cursaru, B. Doicin, S. Mihai, *Dig. J. Nanomater. Bios.* **12**, 483 (2017).
- [7] H. Yu, J. Shen, J. Li, X. Sun, W. Han, X. Liu, L. Wang, *Mater. Lett.* **132**, 259 (2014).
- [8] T. Yutthalekha, C. Wattanakit, C. Warakulwit, W. Wannapakdee, K. Rodponthukwaji, T. Witoon, J. Limtrakul, *J. Clean. Prod.* **142**, 1244 (2017).
- [9] A. K. Jamil, O. Muraza, A. M. Al-Amer, *Particuology* **24**, 138 (2016).
- [10] Y. Liu, L. Xu, Y. Lv, X. Liu, *J. Colloid Interf. Sci.* **479**, 55 (2016).
- [11] S. Alfaro, C. Rodríguez, M.A. Valenzuela, P. Bosch, *Mater. Lett.* **61**, 4655 (2007).
- [12] A. S. Kovo, S. M. Holmes, *J. Dispers. Sci. Technol.* **31**, 442 (2010).
- [13] R. T. Rigo, C. Prigol, Â. Antunes, J. H. Z. dos Santos, S. B. . Pergher, *Mater. Lett.* **102–103**, 87 (2013).
- [14] A. Samadi-Maybodi, S. Masoomeh Pourali, *Micropor. Mesopor. Mat.* **167**, 127 (2013).
- [15] D. Nibou, S. Amokrane, N. Lebaili, *Desalination* **250**, 459 (2010).
- [16] G. Yao, J. Lei, X. Zhang, Z. Sun, S. Zheng, S. Komarneni, *Mater. Res. Bull.* **107**, 132 (2018).
- [17] D. Nibou, H. Mekatel, S. Amokrane, M. Barkat, M. Trari, *J. Hazard. Mater.* **173**, 637 (2010).
- [18] Y. Huang, K. Wang, D. Dong, D. Li, M. R. Hill, A. J. Hill, H. Wang, *Micropor. Mesopor. Mat.* **127**, 167 (2010).
- [19] X. Zhang, D. Tang, M. Zhang, R. Yang, *Powder Technol.* **235**, 322 (2013).
- [20] S. Sivalingam, S. Sen, *Appl. Surf. Sci.* **463**, 190 (2019).
- [21] N. E. Gordina, V. Y. Prokofev, Y. N. Kulpina, N. V. Petuhova, S. I. Gazahova, O. E. Hmylova, *Ultrason. Sonochem.* **33**, 210 (2016).
- [22] E. Yousefi, C. Falamaki, *Chem. Eng. J.* **221**, 247 (2013).
- [23] I. Caballero, F. G. Colina, J. Costa, *Ind. Eng. Chem. Res.* **46**, 1029 (2007).
- [24] S. Askari, S. Alipour, R. Halladj, M. Farahani, *J. Porous Mater.* **20**, 285 (2013).